A Novel Digital FM Receiver for Mobile and Personal Communications

Hyuck M. Kwon, *Senior Member, IEEE*, and Kwang Bok (Ed) Lee, *Member, IEEE*

Abstract— Recently, a digital baseband receiver called zero-intermediate frequency zero-crossing demodulator (ZIFZCD) was developed for digital FM signal detection. ZIFZCD is applicable to many worldwide mobile and personal communications systems. In addition, ZIFZCD offers lower power consumption and simpler implementation, compared to the conventional analog implementation [e.g., a limiter-discriminator integrator and dump (LDI)] and the conventional digital implementation [e.g., the cross-differentiate-multiply demodulator (CDM)]. An objective of this paper is to introduce the ZIFZCD and report the bit-error rate (BER) of the ZIFZCD under both static and fading environments. The analyzed and simulated BER results show that the ZIFZCD is comparable to the conventional CDM for a narrowband digital FM with modulation index 0.5, and the ZIFZCD is significantly better than the CDM for a wideband digital FM with modulation index larger than 1.5.

I. INTRODUCTION

MANY world-wide digital wireless communication systems employ digital frequency modulation (FM) signaling, called continuous phase frequency shift keying (CPFSK). For example, a minimum shift keying (MSK) and a Gaussian minimum shift keying (GMSK) signaling are typical, because of their bandwidth efficiency and their constant envelope properties, which allow the receivers to employ economic class C nonlinear amplifiers [1]. An efficient design of a wireless communication receiver for these digital FM signals has become an important issue.

In general, these FM signals may be demodulated digitally in various ways. The technique in [2] uses the direction of the phase rotation angle to detect signal polarity. A significant problem with this approach is its inability to demodulate multilevel digital FM signals. To overcome this limitation of Ian Vance's receiver, a noncoherent digital FM receiver, called cross-differentiate multiply (CDM) demodulator, has been investigated for first and second-generation digital wireless communication systems [3]. An advantage of the CDM is that bit-error rate (BER) performance is as good as that of the conventional analog limiter-discriminator integrate and dump (LDI) FM receiver. A disadvantage of this CDM demodulator is that the CDM is highly complicated. The number of required devices, hence their electrical current drain, used to realize this technique is undesirable, particularly in battery operated,

H. M. Kwon is with Wichita State University, Department of Electrical Engineering, Wichita, KS 67260-0044 USA (email: hmkwon@ee.twsu.edu).
K. B. Lee is with Seoul National University, School of Electrical Engineering, Seoul, Korea.

portable communication applications. Yet another approach employs the arc-tangent operation like $\tan^{-1}\{q(t)/i(t)\}$ with digitized in-phase $i(t)$ and quadrature-phase $q(t)$ signals [4]. This technique requires two multibit analog-to-digital (A/D) converters and a multibit processor. Once again the current drain is undesirable, particularly in portable applications.

Another conventional digital FM demodulator has been developed for satellite application [5]. A nonzero-IF digital FM signal is directly one-bit A/D sampled at the receiver front end. The FM discriminator function is approximated by observing the difference between the one-bit A/D converted samples. Whenever the sign of the sample value changes from $+1$ to -1 (or from -1 to $+1$), a zero crossing pulse is generated. Then a counter sums the total number of zero-crossings per symbol time. A symbol-by-symbol decision is made by comparing the counter output with thresholds. Unfortunately, this receiver employs a single phase axis generator, i.e., only $i(t)$, and works for only a wideband digital FM signal with modulation index larger than 1 (because there may be no zero-crossings for a symbol interval when FM modulation index is small, such as 1/2). In other words, this scheme does not work for many world-wide mobile communication systems because the $\pi/4$-differential quadrature phase shift keying (DQPSK) and the GMSK employ modulation indices less than or equal to 1/2. The narrowband digital FM and $\pi/4$-DQPSK receivers require more than two phase components.

Recently, an efficient baseband receiver, called zero-intermediate frequency zero-crossing demodulator (ZIFZCD), was developed for implementation of a digital-FM receiver [6], [7]. This ZIFZCD can easily generate multiple phase components and detect the zero-crossings of each phase component. Thus, this ZIFZCD can demodulate both narrowband and wideband digital FM signals, and is applicable to many world-wide mobile communication systems. Another advantage of the ZIFZCD is that its complexity is much lower, implementation is simpler, and power consumption is smaller than those of the conventional schemes. Furthermore, the spurious components can be significantly reduced by employing a direct zero-IF conversion, and receivers based on the zero-IF potentially offer easy integration of receiver components and programmable bandwidth benefits, compared to receivers based on nonzero-IF [8]. No analysis was performed in [7] and only simulation results under a static environment were presented for a narrowband digital FM signal.

An objective of this paper is to introduce the ZIFZCD and to analyze and simulate the BER performance of this ZIFZCD under both static and fading environments. In addition, in this paper both narrowband and wideband digital FM signals will

be applied to the ZIFZCD, and performance of the ZIFZCD will be compared with that of the conventional CDM.

Section II describes the system model and Section III presents the ZIFZCD. Section IV analyzes the performance of the ZIFZCD under static and fading environments. Section V presents numerical results. Finally, Section VI presents conclusions.

II. SYSTEM MODEL

The transmitted digital FM signal $s(t)$ can be written as

$$
s(t) = \sqrt{2P} \cos \left(2\pi f_c t + 2\pi f_d \int_{-\infty}^{t} \sum_{n=-\infty}^{\infty} a_n d(\tau - nT_s) d\tau \right) \tag{1}
$$

where P is the signal power, f_c the carrier frequency, f_d the frequency deviation, $a_n = \pm 1$ binary data, and $d(t)$ the rectangular pulse over a symbol (or bit) time $T_s, 0 \leq t \leq T_s$. Both additive white Gaussian noise (AWGN), i.e., static, and Rayleigh Doppler frequency shifted fading environments are considered. The carrier recovery, required for coherent detection, is difficult in mobile, fading environments. A noncoherent scheme provides superior performance in Rayleigh fading environments, compared to coherent detection. This paper assumes a noncoherent digital FM receiver. The receiver employs a Gaussian intermediate frequency (IF) filter of bandwidth time product $B_r T$. The FM modulation index (the peak-to-peak frequency deviation $2f_d$ normalized by the symbol rate $1/T_s$) is denoted by $h = 2f_d T_s$. The CPFSK signal becomes an MSK when h is 1/2.

The received signal at the input to the IF filter in a conventional LDI receiver is written as

$$
x(t) = R(t) \cos(2\pi f_{\mathrm{IF}} t + \theta(t) + \delta(t)) + n_w(t) \tag{2}
$$

under Rayleigh fading and static environments where $R(t)$ is the received Rayleigh fading envelope, $\delta(t)$ the Rayleigh fading phase, f_{IF} the center frequency of the IF filter, $n_w(t)$ the AWGN with one-sided spectral density N_0, and $\theta(t)$ the data phase after FM modulation given by

$$
\theta(t) = \frac{\pi h}{T_s} \int_{-\infty}^{t} \sum_{n=-\infty}^{\infty} a_n d(\tau - nT_s) d\tau. \tag{3}
$$

The Rayleigh fading envelope $R(t)$ and phase $\delta(t)$ are assumed to vary slowly compared to the data rate. The complex equivalent low-pass Rayleigh fading process can be written as $R(t)e^{j\delta(t)} = x_{\mathrm{fade}}(t) + jy_{\mathrm{fade}}(t)$ where $x_{\mathrm{fade}}(t)$ and $y_{\mathrm{fade}}(t)$ are the in-phase and quadrature-phase components of the fading process, respectively. The $x_{\mathrm{fade}}(t)$ and $y_{\mathrm{fade}}(t)$ are Gaussian processes with the following power spectral densities

$$
S_{x_{\mathrm{fade}}}(f) = S_{y_{\mathrm{fade}}}(f) = \begin{cases} \dfrac{\sigma_s^2}{\pi \sqrt{f_D^2 - f^2}} & |f| \leq f_D \\ 0 & \text{elsewhere} \end{cases} \tag{4}
$$

where σ_s^2 is the power of the Rayleigh fading process and f_D is the Doppler frequency shift. The low-pass equivalent transfer function of the IF filter is denoted by $H(f)$. The IF filter bandlimits $x(t)$, which results in a time-varying signal envelope $R(t)a(t)$, a distorted signal phase $\phi(t)$ due to the intersymbol interference (ISI), and a signal-dependent phase noise $\eta(t)$ where $a(t)$ is the filtered signal amplitude whose square is

$$
a^2(t) = \left(\int_{-\infty}^{t} h(t - \tau) \cos \theta(\tau) d\tau \right)^2 + \left(\int_{-\infty}^{t} h(t - \tau) \sin \theta(\tau) d\tau \right)^2. \tag{5}
$$

The output of the IF bandpass filtered noise, $n(t)$, can be represented as

$$
n(t) = n_c(t) \cos 2\pi f_{\mathrm{IF}} t + n_s(t) \sin 2\pi f_{\mathrm{IF}} t \tag{6}
$$

where the variance of the $n_c(t)$ and $n_s(t)$ are equal to the $N_0 B$ where B is the low-pass equivalent two-sided noise bandwidth. The output of the bandpass limiter can be written as

$$
y(t) = \cos(2\pi f_{\mathrm{IF}} t + \phi(t) + \delta(t) + \eta(t)) \tag{7}
$$

where the distorted signal phase can be written as

$$
\phi(t) = \tan^{-1} \frac{\int_{-\infty}^{t} h(t - \tau) \sin \theta(\tau) d\tau}{\int_{-\infty}^{t} h(t - \tau) \cos \theta(\tau) d\tau} \tag{8}
$$

and the phase noise $\eta(t)$ as

$$
\eta(t) = \tan^{-1} \frac{\sqrt{2\rho(t)} \sin \phi(t) + \xi(t)}{\sqrt{2\rho(t)} \cos \phi(t) + \zeta(t)}. \tag{9}
$$

The $\xi(t)$ and $\zeta(t)$ in (9) are independent Gaussian random variables with zero mean and unit variance, and $\rho(t)$ is the time varying signal-to-noise ratio (SNR) given by

$$
\rho(t) = \frac{R^2(t)}{N_0} \frac{a^2(t)}{T_s \int_{\infty}^{-\infty} |H(f)|^2 df} = \frac{R^2(t)}{N_0} \frac{a^2(t)}{BT_s}. \tag{10}
$$

The transmitted data information $d(t)$ is imbedded at $\phi(t)$ in (8). The receiver estimates data information $d(t)$ by using the phase of the limiter output signal. If the impulse response of the filter is the Dirac delta function, the phase $\phi(t)$ becomes the undistorted signal phase $\theta(t)$ from (8). The output of the conventional discriminator is the derivative of the phase $\phi(t) + \eta(t) + \delta(t)$. The integrate and dump filter, following the discriminator, reintegrates this derivative $d(\phi(t) + \eta(t) + \delta(t))/dt$ over the current symbol time interval, producing a phase difference $\Delta\Phi(t) = \Delta\phi(t) + \Delta\eta(t) + \Delta\delta(t)$ where $\Delta\phi(t) = \phi(t) - \phi(t - T_s)$, $\Delta\eta(t) = \eta(t) - \eta(t - T_s)$, and $\Delta\delta(t) = \delta(t) - \delta(t - T_s)$. The receiver chooses "1" b if the phase difference $\Delta\Phi(t)$ is positive, and "0" b otherwise for a binary-level CPFSK signal.

The closed expression of the cumulative distribution function of the random variable

$$
\Delta\psi(t) \equiv \Delta\eta(t) + \Delta\delta(t) \tag{11}
$$

was recently published in [9] for the modulation index $h \leq 1.5$ by employing the results in [10]. For convenience, the
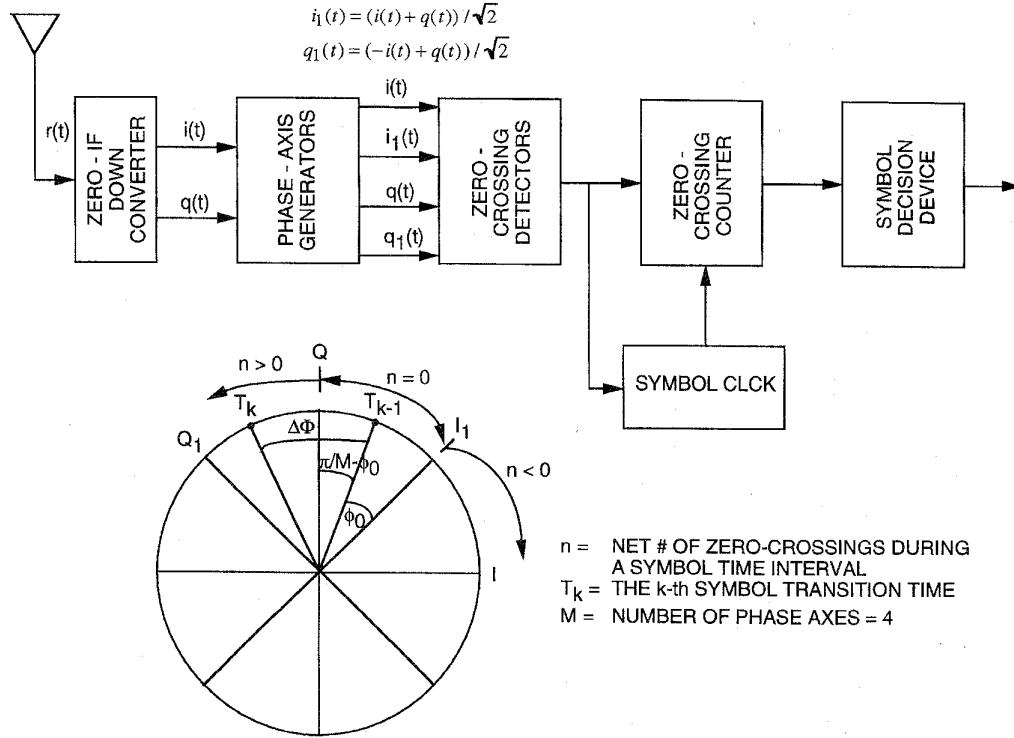
Fig. 1.   Block diagram of a zero-IF zero-crossing demodulator (ZIFZCD). Example of initial phase ϕ_0, and phase zones corresponding to positive, zero, and negative n (the net number of zero crossings for a symbol time interval).

distribution function is repeated here as follows:

$$F(\Delta\psi) = \frac{1}{2\pi} \left[\Delta\psi + \pi + \frac{\phi_T \sin \Delta\psi}{\sqrt{1 - \phi_T^2 \cos^2 \Delta\psi}} \right.$$

$$\left. \times \left\{ \frac{\pi}{2} + \sin^{-1}(\phi_T \cos \Delta\psi) \right\} \right] \quad (12)$$

where ϕ_T is an autocorrelation coefficient of the combined Gaussian process which takes into account ISI due to the IF filter. The ϕ_T can be written as

$$\phi_T = J_0(2\pi f_D T_s) \sqrt{\frac{C_1^2 - C_2^2}{(C_1 + 1/\rho)^2 - C_2^2}} \quad (13)$$

where $J_0(x)$ is the zeroth-order Bessel function of the first kind

$$C_1 = \frac{1}{2} \left[a^2(t_0) + a^2(t_0 - T_s) \right] \quad (14)$$

$$C_2 = \frac{1}{2} \left[a^2(t_0) - a^2(t_0 - T_s) \right] \quad (15)$$

and ρ is the SNR of the multipath signal power σ_s^2 over the Gaussian noise power σ_n^2 at the IF filter output. The SNR ρ can be written as

$$\rho = \frac{\sigma_s^2}{\sigma_n^2} = \frac{\sigma_s^2 T_s}{\sigma_n^2 T_s} = \frac{E_s}{N_0 B T_s} = \frac{E_b}{N_0 B T_b} \quad (16)$$

for the binary system where E_b is the average received multipath signal bit energy at the receiver input.

Two baseband signals, the in-phase signal $i(t)$ and the quadrature-phase signal $q(t)$, which are created by either direct conversion or mixing the bandlimitted IF signal with $\cos(2\pi f_{IF} t)$ and $\sin(2\pi f_{IF} t)$, can be written as

$$i(t) = \cos(\phi(t) + \delta(t) + \eta(t)) \quad (17)$$

and

$$q(t) = \sin(\phi(t) + \delta(t) + \eta(t)). \quad (18)$$

III. ZIFZCD

The ZIFZCD's consist of four parts, as shown in Fig. 1; phase axis generators, zero-crossing detectors, zero-crossing counter, and symbol decision device.

A. Phase Axis Generator

The inputs to the phase axis generator are the in-phase $i(t)$ and quadrature-phase $q(t)$ components of a downconverted CPFSK signal. The phase trajectory in a phasor domain crosses I and Q phase axes whenever the $i(t)$ and $q(t)$ signals cross the zero axis in the time domain, respectively. The additional phase axes I_1 and Q_1 can be easily generated by employing only I and Q. For example, the signal $i_1(t)$, which is associated with I_1 phase axis, is a sum of $i(t)$ and $q(t)$ with scaling $1/\sqrt{2}$, and can be written as

$$i_1(t) = (i(t) + q(t))/\sqrt{2}$$
$$= \cos(\phi(t) + \eta(t) + \delta(t) - \pi/4). \quad (19)$$

Similarly the $q_1(t)$ can be written as

$$q_1(t) = (-i(t) + q(t))/\sqrt{2}$$
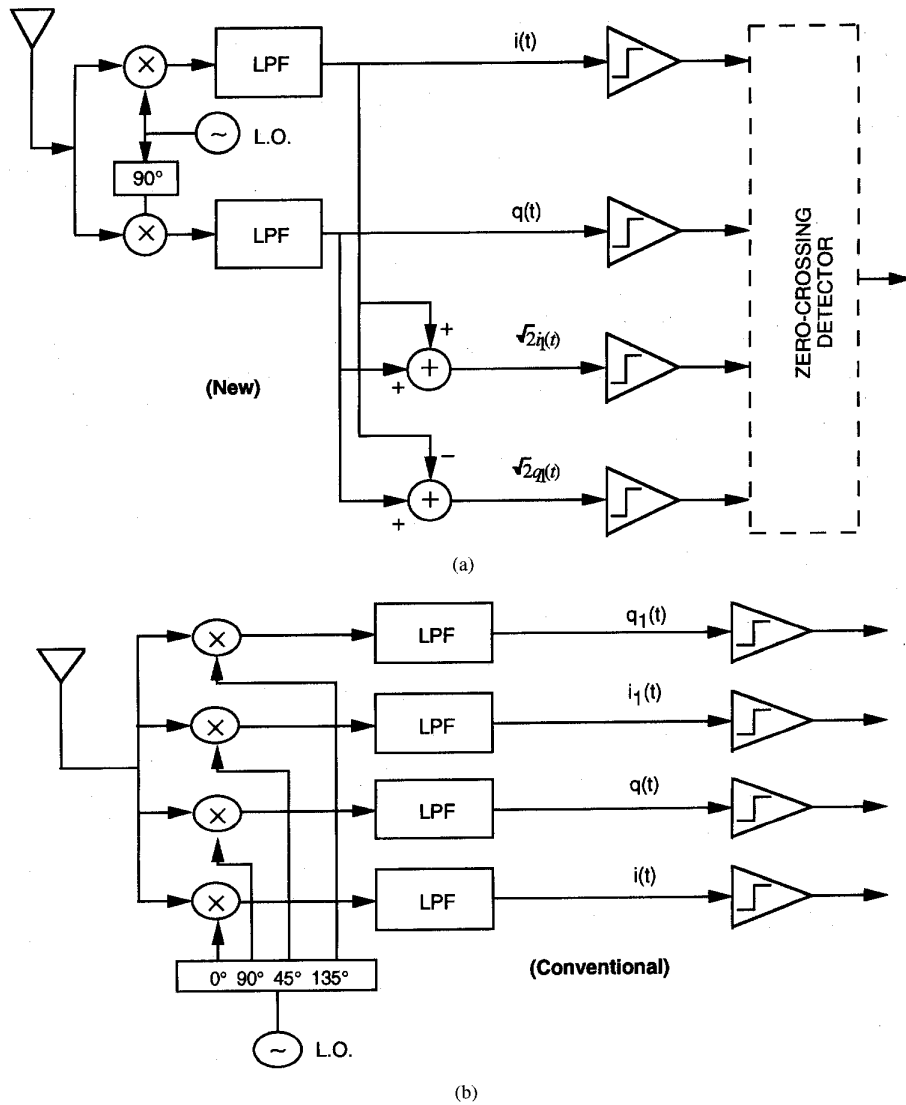$$= \sin(\phi(t) + \eta(t) + \delta(t) - \pi/4). \quad (20)$$

Fig. 2. (a) A novel multiple phase axis generator and (b) a conventional multiple phase axis generator for $M = 4$ axes.

The phase axis generator using (19) and (20) requires only two summers and two scalers with $i(t)$ and $q(t)$ inputs while the conventional phase axes generator needs phase splitters and additional mixers, which is much more complicated than the new scheme. See Fig. 2 for comparisons. More than four phase axes can be generated by combinations of adding and subtracting $i(t)$, $q(t)$, $i_1(t)$, $q_1(t)$, and their descendants. The output of the mth phase axis generator is denoted by $i_m(t)$ and $q_m(t)$, m an integer, $0 \leq m \leq M/2 - 1$ where M is the total number of phase axes, and $i_0(t)$ and $q_0(t)$ denote $i(t)$ and $q(t)$, respectively.

B. Zero-Crossing Detector

Each zero-crossing detector (ZCD) takes a pair of signals, $i_m(t)$ and $q_m(t)$, from the phase axis generator output, and detects zero-crossings (i.e., phase axis-crossing time points) and the phase-rotation directions of each signal. So, $M/2$ ZCD's are necessary for the detection of zero-crossing points from all M signals. If the $i_m(t)$ signal changes its value from

positive to negative and the value of $q_m(t)$ at the crossing time is negative, then the $i_m(t)$-zero-crossing detector generates a negative pulse at the crossing time in order to indicate that the estimated phase rotation is in a clockwise direction, and vice-versa. The output of the ZCD employing $i_m(t)$ and $q_m(t)$, denoted by $z_{I_m Q_m}(k)$, can be written as

$$z_{I_m Q_m}(k) = i_{h,m}(k)(q_{h,m}(k) - q_{h,m}(k - 1)) \\ - q_{h,m}(k)(i_{h,m}(k) - i_{h,m}(k - 1)) \quad (21)$$

where $i_{h,m}(k)$ and $q_{h,m}(k)$ are the one-bit A/D outputs when inputs to the hardlimiters are $i_m(t)$ and $q_m(t)$, respectively, and k denotes the kth sample time point. The number of samples per symbol is denoted by N_s. This ZCD requires only two one-bit A/Ds, two delay units, three binary adders, and two-binary multiplication for a pair of $i_m(t)$ and $q_m(t)$ signals.

However, in the conventional CDM, the discrimination, i.e., the derivative of the sum of signal phase $\phi(t)$, the noise phase $\eta(t)$, and the Rayleigh fading phase $\delta(t)$, is implemented by
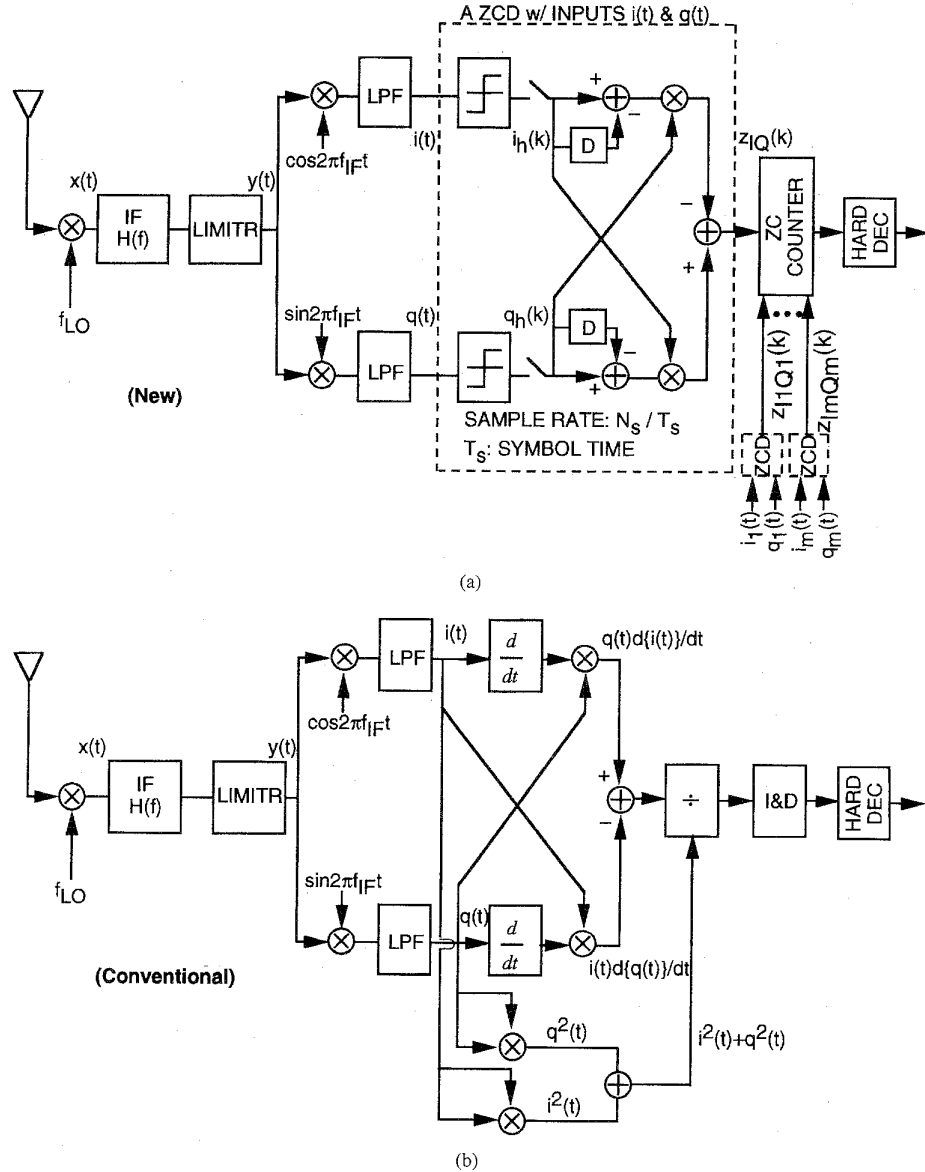
Fig. 3. (a) A novel ZCD and (b) a CDM demodulator with two phase axes $i(t)$ and $q(t)$ for a CPFSK signal.

employing $i(t)$ and $q(t)$ as

$$\frac{d}{dt}\{\phi(t) + \eta(t) + \delta(t)\} = \frac{i(t)\frac{d}{dt}q(t) - q(t)\frac{d}{dt}i(t)}{i^2(t) + q^2(t)} \qquad (22)$$

because $\phi(t) + \eta(t) + \delta(t)$ can be written as

$$\phi(t) + \eta(t) + \delta(t) = \tan^{-1}\left(\frac{q(t)}{i(t)}\right). \qquad (23)$$

This conventional CDM requires two differentiators, four multipliers, one divider, and two summers. A digital implementation of the CDM requires two multibit (typically eight-bits) A/D converters, discrimination components, and either a microprocessor or digital signal processor. Therefore, the complexity of the ZCD is significantly simpler than that of the conventional CDM. See Fig. 3 for comparisons.

C. Symbol Synchronization for ZCD

In practical applications, the local clock, which generates the reference times, exhibits time-jittering phenomena. Therefore, the clock reference time should be updated. In other words, symbol synchronization before symbol decision should be acquired and updated accurately. A simple symbol synchronization algorithm has been simulated under static environment by the authors [11]. It was observed that the symbol synchronization loss is insignificant, e.g., less than 0.2 dB for E_b/N_0 from 0 dB to 14 dB. Thus, perfect symbol synchronization will be assumed in this paper.

D. Zero-Crossing Counter

The zero-crossing counter sums the total number of positive (n^+) and negative (n^-) binary pulses with signs coming from $M/2$ ZCD's over one symbol time, i.e., $n = n^+ - n^-$, which

can be written as

$$n = \sum_{k=1}^{N_s} \sum_{m=0}^{M/2-1} z_{I_m Q_m}(k) \qquad (24)$$

where the value of $z_{I_m Q_m}(k)$ in (21) and (24) is ± 1 or 0. The number of net zero-crossings, n, is linearly proportional to the total phase rotation angle, $\Delta\Phi = \Delta\phi + \Delta\eta + \Delta\delta$, for symbol time T_s.

E. Symbol Decision Device

The symbol decision device measures the magnitude and the sign of the zero crossing counter output and compares them with the thresholds to make a symbol decision. Binary-level transmission employs one threshold which is zero. A hard decision rule for a binary transmission can be written as

$$\hat{d}(k) = \begin{cases} \text{`1'} & \text{bit} & \text{if } n > 0 \\ \text{random decision `0' or `1'} & \text{if } n = 0. \\ \text{`0'} & \text{bit} & \text{if } n < 0 \end{cases} \qquad (25)$$

The decision rule given by (25) can be easily modified for multilevel transmission.

IV. BER ANALYSIS

A. BER of ZIFZCD for Narrowband FM Under Fading Environment

Let ϕ_0 denote the phase angle between a symbol starting point and the nearest phase axis in the opposite direction to the rotation, $0 \le \phi_0 \le \pi/M$ (see Fig. 1). Let N denote the number of "clicks" in the time interval $(t-T_s, t)$ [10]. Suppose that there is no click during a symbol time, i.e., $N = 0$, and "1" b was transmitted. When the overall phase rotation over one symbol time, $\Delta\Phi$, is less than $-\phi_0$, then the net number of zero-crossings is negative and a bit error occurs. When $\Delta\Phi$ is larger than $-\phi_0$ and less than $(\pi/M - \phi_0)$, the net number of zero-crossings is zero and a bit error may occur with 1/2 probability due to a random bit decision. Let $P_{\text{cont}}(e \mid \phi_0, N = 0)$ denote the conditional bit error probability given ϕ_0 and no clicks. Then, $P_{\text{cont}}(e \mid \phi_0, N = 0)$ can be written as

$$P_{\text{cont}}(e \mid \phi_0, N = 0) = \Pr[n < 0 \mid \phi_0, N = 0]$$
$$+ \frac{1}{2}\Pr[n = 0 \mid \phi_0, N = 0] \qquad (26)$$

where

$$\Pr[n < 0 \mid \phi_0, N = 0]$$
$$= \Pr[\Delta\phi - \pi < \Delta\Phi \equiv \Delta\phi + \Delta\eta + \Delta\delta$$
$$= \Delta\phi + \Delta\psi \le -\phi_0]$$
$$= \Pr[-\pi < \Delta\psi \le -\phi_0 - \Delta\phi]$$
$$= F(-\phi_0 - \Delta\phi) - F(-\pi), \qquad (27)$$
$$\Pr[n = 0 \mid \phi_0, N = 0]$$
$$= \Pr\left[-\phi_0 < \Delta\phi + \Delta\psi \le \frac{\pi}{M} - \phi_0\right]$$
$$= \Pr\left[-\phi_0 - \Delta\phi < \Delta\psi \le \frac{\pi}{M} - \phi_0 - \Delta\phi\right]$$
$$= F\left(\frac{\pi}{M} - \phi_0 - \Delta\phi\right) - F(-\phi_0 - \Delta\phi) \qquad (28)$$

and $\Delta\psi = \Delta\eta + \Delta\delta$ and $F(x)$ is expressed in (12). Note that $F_\psi(x)$ in [12] is the probability distribution function of $\psi \equiv (\Delta\phi + \Delta\eta) \bmod (2\pi)$ under static environment, including the signal phase change $\Delta\phi$ while $F(x)$ in (12) and (28) is the distribution function of phase-noise change $\Delta\eta$ plus fading-phase change $\Delta\delta$ under fading and static environments, excluding the signal phase change $\Delta\phi$. Using $F(-\pi) = $ zero in (27), the conditional bit error probability given ϕ_0 for the no click noise case can be rewritten as

$$P_{\text{cont}}(e \mid \phi_0, N = 0)$$
$$= \frac{1}{2}\left(F(-\phi_0 - \Delta\phi) + F\left(\frac{\pi}{M} - \phi_0 - \Delta\phi\right)\right). \qquad (29)$$

For a narrowband CPFSK, the overall bit error probability, including click noise, can be written as

$$P_b(E \mid \phi_0) = \Pr(N = 0)P_{\text{cont}}(e \mid \phi_0, N = 0)$$
$$+ \{1 - \Pr(N = 0)\}$$
$$= e^{-\bar{N}}P_{\text{cont}}(e \mid \phi_0, N = 0) + 1 - e^{-\bar{N}} \qquad (30)$$

where $\bar{N}$ is the average number of clicks over a symbol duration, which can be written as

$$\bar{N} = \frac{1}{2\pi\rho} \int_{t_0-T_s}^{t_0} \frac{\phi(t)}{a^2(t) + 1/\rho} dt \qquad (31)$$

for the Rayleigh fading channel. Using (29)–(31), the overall bit error probability of the ZIFZCD under fading can be computed as

$$P_b(E) = \frac{1}{\pi/M} \int_0^{\pi/M} P_b(E \mid \phi_0) d\phi_0. \qquad (32)$$

The BER of the CDM under fading is a special case of the BER of the ZIFZCD with $\phi_0 = 0$ and $M = \infty$ in (30). The signal phase change $\Delta\phi$ and the average number of clicks $\bar{N}$ depend on the transmitted data pattern due to the ISI. Typically, four data bit patterns, i.e., 111, 110, 011, and 010, determine the values of $\Delta\phi$ and $\bar{N}$ when the currently transmitted bit is "1" b and located at the middle position of the pattern. The overall bit error rate is the average of the BER in (32) over the possible data patterns.

B. BER of ZIFZCD for Narrowband FM Under Static Environment

If the channel is under only static environment, the BER can be derived from that of the fading case by replacing $R(t)$ and $\delta(t)$ in (2) with $\sqrt{2P}$ and 0, respectively. By defining ψ to be the principle angle of the $\Delta\Phi$, i.e.,

$$\psi \equiv (\Delta\phi + \Delta\eta)\bmod(2\pi), \quad \Delta\phi - \pi < \psi \le \Delta\phi + \pi \qquad (33)$$

$P_{\text{cont}}(e \mid \phi_0, N = 0)$ can be written as

$$P_{\text{cont}}(e \mid \phi_0, N = 0) = \Pr[n < 0 \mid \phi_0, N = 0]$$
$$+ \frac{1}{2}\Pr[n = 0 \mid \phi_0, N = 0] \qquad (34)$$

where

$$
\begin{aligned}
\Pr[n < 0 \mid \phi_0, N = 0] &= \Pr[\Delta\phi - \pi < \psi \leq -\phi_0] \\
&= F_\psi(-\phi_0) - F_\psi(\Delta\phi - \pi) \quad (35)
\end{aligned}
$$

$$
\begin{aligned}
\Pr[n = 0 \mid \phi_0, N = 0] &= \Pr\left[-\phi_0 < \psi \leq \frac{\pi}{M} - \phi_0\right] \\
&= F_\psi\left(\frac{\pi}{M} - \phi_0\right) - F_\psi(-\phi_0) \quad (36)
\end{aligned}
$$

and $F_\psi(x)$ is given by [12, (9)]. Note that $F_\psi(\Delta\phi - \pi)$ is zero. The conditional bit error probability in (34), given ϕ_0 and no clicks, can be rewritten as

$$
P_{\text{cont}}(e \mid \phi_0, N = 0) = \frac{1}{2}\left(F_\psi(-\phi_0) + F_\psi\left(\frac{\pi}{M} - \phi_0\right)\right). \quad (37)
$$

The conditional bit error probability, given ϕ_0 including click noise, can be written as in (30) where $\bar{N}$ is the average number of positive clicks over a symbol duration which is given by [10, eqs. (21), (22), (24), (31)]. The overall bit error probability of the ZIFZCD is found as in (32).

C. BER of ZIFZCD for Wideband Digital FM With $h = 1.5$ Under Static Environment

The $F_\psi(x)$ given by [12, (9)] has been used for the narrowband CPFSK BER analysis, and note that $F_\psi(x)$ is an approximation for the modulation index h less than 1.5. If h is less than one, the approximation is accurate. If h is larger than one, then the approximation becomes less accurate. For large h, the closed form of the BER expression has not been available in the literature to the authors' knowledge. In this paper $F_\psi(x)$ is employed for the ZIFZCD BER analysis even though $F_\psi(x)$ is not accurate with $h = 1.5$.

The shaded and dotted areas in Fig. 4(a) show the two ZIFZCD error events for $n < 0$ and $n = 0$, respectively, for "1" b transmission in "111" data pattern and initial phase ϕ_0, $0 \leq \phi_0 \leq \pi/M$. The $\Delta\phi$ is $\pi h \, (= 1.5\pi)$, and $\Delta\phi - \pi \, (= 0.5\pi)$ is positive and larger than $\pi/M - \phi_0$ for $M \geq 4$ when data pattern is "111." The conditional probabilities that $n < 0$ and $n = 0$, respectively, given "111" pattern and initial phase ϕ_0, can be written as

$$
\begin{aligned}
&\Pr[n < 0 \mid \text{'111'}, \phi_0] \\
&= \Pr[-\infty < \Delta\phi_{111} + \Delta\eta \leq -\phi_0] \\
&= 1 - e^{-\bar{N}_{111}} - \bar{N}_{111}e^{-\bar{N}_{111}} \\
&\quad \times \{F_\psi(2(\Delta\phi_{111} - \pi) + \phi_0) - F_\psi(\Delta\phi_{111} - \pi)\} \quad (38)
\end{aligned}
$$

and

$$
\begin{aligned}
&\Pr[n = 0 \mid \text{'111'}, \phi_0] \\
&= \Pr\left[-\phi_0 < \Delta\phi_{111} + \Delta\eta \leq \frac{\pi}{M} - \phi_0\right] \\
&= \bar{N}_{111}e^{-\bar{N}_{111}}\{F_\psi(2(\Delta\phi_{111} - \pi) + \phi_0) \\
&\quad - F_\psi(2(\Delta\phi_{111} - \pi) - (\pi/M - \phi_0))\}. \quad (39)
\end{aligned}
$$

In (38) and (39), it is assumed that the probability density function (pdf) of the overall phase change, $P_{\Delta\Phi}(x)$, for $\Delta\phi - 3\pi \leq x \leq \Delta\phi - \pi$ region, is equal to $\Pr[N = 1]$ times $p_\psi(x + 2\pi)$, and $p_\psi(x)$ is symmetric around $\Delta\phi$. These assumptions were employed in the narrowband analysis [10],

[12]. The conditional bit error probability given data pattern "111" and initial phase ϕ_0 can be calculated as

$$
\begin{aligned}
P_b(E \mid \text{'111'}, \phi_0) &= \Pr[n < 0 \mid \text{'111'}, \phi_0] \\
&\quad + \frac{1}{2}\Pr[n = 0 \mid \text{'111'}, \phi_0] \quad (40)
\end{aligned}
$$

using (30) and (31). The conditional BER given data pattern, $P_b(E \mid \text{'1111'})$, is given by

$$
P_b(E \mid \text{'111'}) = \frac{1}{\pi/M}\int_0^{\pi/M} P_b(E \mid \text{'111'}, \phi_0)d\phi_0. \quad (41)
$$

The conditional BER of the LDI, given data pattern "111," is that of the ZIFZCD with $\phi_0 = 0$ and $M = \infty$ in (40). The error event area for the LDI, i.e., $-\infty < \Delta\Phi \leq 0$ region in Fig. 4(a), can be larger than that for the ZIFZCD from the convex property of the probability distribution when h is large such as 1.5 and "111" data pattern is transmitted. It is assumed that $p_\psi(x)$ is in a bell shape in Fig. 4(a). This is an unexpected result because the ZIFZCD can be regarded as a quantized version of the LDI from the rotation angle estimation point of view, and the. quantized version is in general expected to be worse than the unquantized one. For this case, the quantization error results in the ZIFZCD superior to the LDI when the phase change $\Delta\Phi$ is less than $(\Delta\phi - \pi)$ and larger than $(\Delta\phi + \pi)$. Some simulation results in the next section also verify that the ZIFZCD can be better than the LDI if the modulation index is large such as $h \geq 1.5$.

Fig. 4(b) and (c) show the error events of the ZIFZCD corresponding to data pattern "010." The ISI can be significant when data pattern is "010" because of the a.c. characteristics in the data pattern and the narrowband IF filter. The signal phase change $\Delta\phi_{010}$ is only 0.879π due to the ISI instead of 1.5π when the IF filter is a Gaussian filter with B_rT equal to 1 and $h = 1.5$. Thus, $\Delta\phi_{010} - \pi$ is less than zero. The integral interval in (41) should be divided into two parts depending on ϕ_0 in (32). Fig. 4(b) and (c) show the two cases: (1) $\Delta\phi_{010} - \pi \leq -\phi_0$, i.e., $0 < \phi_0 \leq \pi - \Delta\phi_{010} = 0.121\pi$, and (2) $-\phi_0 < \Delta\phi_{010} - \pi \leq \pi/M - \phi_0$, i.e., $\pi - \Delta\phi_{010} = 0.121\pi < \phi_0 \leq \pi/M$, respectively. When $0 < \phi_0 \leq \pi - \Delta\phi_{010}$, from Fig. 4(b)

$$
\begin{aligned}
&\Pr[n < 0 \mid \text{'010'}, \phi_0, \text{Case}(1)] \\
&= \Pr[-\infty < \Delta\phi_{010} + \Delta\eta \leq -\phi_0] \\
&= e^{-\bar{N}_{010}}\{F_\psi(-\phi_0) - F_\psi(\Delta\phi_{010} - \pi)\} + 1 - e^{-\bar{N}_{010}} \quad (42)
\end{aligned}
$$

and

$$
\begin{aligned}
&\Pr[n = 0 \mid \text{'010'}, \phi_0, \text{Case}(1)] \\
&= \Pr[-\phi_0 < \Delta\phi_{010} + \Delta\eta \leq \pi/M - \phi_0] \\
&= e^{-\bar{N}_{101}}\{F_\psi(\pi/M - \phi_0) - F_\psi(-\phi_0)\}. \quad (43)
\end{aligned}
$$

The conditional BER, given a "010" data pattern and ϕ_0 for case (1), is given by

$$
\begin{aligned}
&P_b(E \mid \text{'010'}, \phi_0, \text{Case}(1)) \\
&= \Pr[n < 0 \mid \text{'010'}, \phi_0, \text{Case}(1)] \\
&\quad + 1/2\Pr[n = 0 \mid \text{'010'}, \phi_0, \text{Case}(1)]. \quad (44)
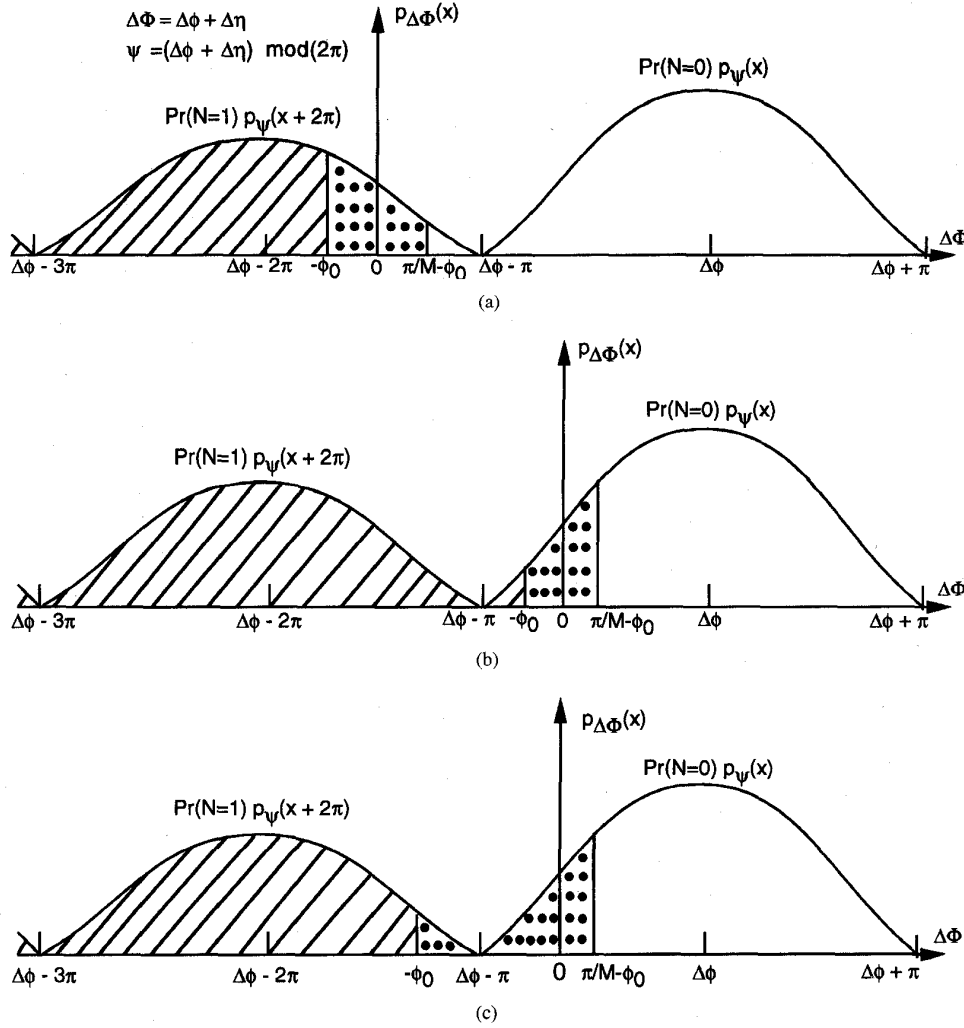\end{aligned}
$$

Fig. 4. The shaded and dotted area demonstrate an example of the probability that $n < 0$ and $n = 0$, respectively: (a) $\pi/M - \phi_0 < \Delta\phi - \pi$ for "111" data pattern where $\Delta\phi_{111} = \pi h = 1.5\pi$, (b) $\Delta\phi - \pi < -\phi_0 \le 0$ for "010" data pattern where $\Delta\phi_{010}$ is 0.879π, and (c) $-\phi_0 < \Delta\phi - \pi \le 0$ for "010" data pattern. $M = 4$, $h = 1.5$, and a Gaussian shape IF filter of $B_r T = 1$ were assumed.

When $\pi - \Delta\phi_{010} < \phi_0 \le \pi/M$, from Fig. 4(c)

$$\Pr[n < 0 \mid \text{`010'}, \phi_0, \text{Case}(2)]$$

$$= \Pr[-\infty < \Delta\phi_{010} + \Delta\eta \le -\phi_0] = \bar{N}_{010} e^{-\bar{N}_{010}}$$

$$\times [1 - \{F_\psi(2(\Delta\phi_{010} - \pi) + \phi_0) - F_\psi(\Delta\phi_{010} - \pi)\}]$$

$$+ 1 - e^{-\bar{N}_{010}} - \bar{N}_{010} e^{-\bar{N}_{010}} \tag{45}$$

and

$$\Pr[n = 0 \mid \text{`010'}, \phi_0, \text{Case}(2)]$$

$$= \Pr[-\phi_0 < \Delta\phi_{010} + \Delta\eta \le \pi/M - \phi_0]$$

$$= \bar{N}_{010} e^{-\bar{N}_{010}} \{F_\psi(2(\Delta\phi_{010} - \pi) + \phi_0) - F_\psi(\Delta\phi_{010} - \pi)\}$$

$$+ \left(e^{-\bar{N}_{010}}\right) \{F_\psi(\pi/M - \phi_0) - F_\psi(\Delta\phi - \pi)\}. \tag{46}$$

The conditional BER, given a "010" data pattern and ϕ_0 for case (2), is given by

$$P_b(E \mid \text{`010'}, \phi_0, \text{Case}(2))$$

$$\Pr[n < 0 \mid \text{`010'}, \phi_0, \text{Case}(2)]$$

$$+ 1/2\Pr[n = 0 \mid \text{`010'}, \phi_0, \text{Case}(2)]. \tag{47}$$

The conditional BER, given a "010" data pattern, can be written as

$$P_b(E \mid \text{`010'})$$

$$= \frac{1}{\pi/M} \left\{ \int_0^{\pi - \Delta\phi_{010}} P_b(E \mid \text{`010'}, \phi_0, \text{Case}(1)) d\phi_0 \right.$$

$$\left. + \int_{\pi - \Delta\phi_{010}}^{\pi/M} P_b(E \mid \text{`010'}, \phi_0, \text{Case}(2)) d\phi_0 \right\}. \tag{48}$$

The conditional BER of the LDI, given a "010" data pattern, is given by (42) with $\phi_0 = 0$.

The conditional BER of the ZIFZCD, given a "110" data pattern, is a mixed case of the "111" and "010". The signal phase change $\Delta\phi_{110}$ is $(\Delta\phi_{111} + \Delta\phi_{010})/2 = 1.19\pi$ due to the ISI instead of 1.5π when the IF filter is a Gaussian filter with $B_r T$ equal to 1 and $h = 1.5$. The lower edge of the principal angle, $\Delta\phi - \pi$, is larger than zero. If M is 4, then $(\pi/M - \phi_0) \le 0.25\pi$ can be larger than $\Delta\phi_{110} - \pi = 0.19\pi$. The integral interval with respect to ϕ_0 for the average BER
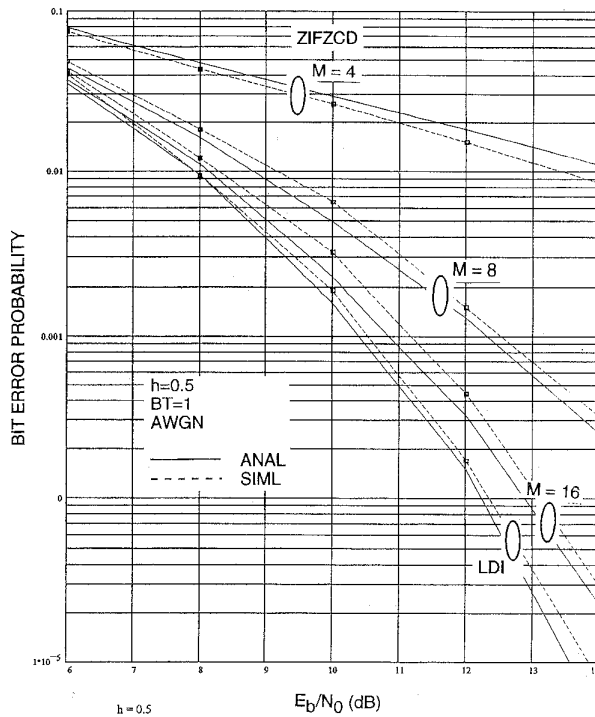
Fig. 5. BER of the ZIFZCD under static environment, with the number of phase axes M as a parameter, $M = 4$, 8, and 16. A narrowband CPFSK with modulation index $h = 0.5$ and a Gaussian shape IF filter of $B_r T = 1$ were assumed.
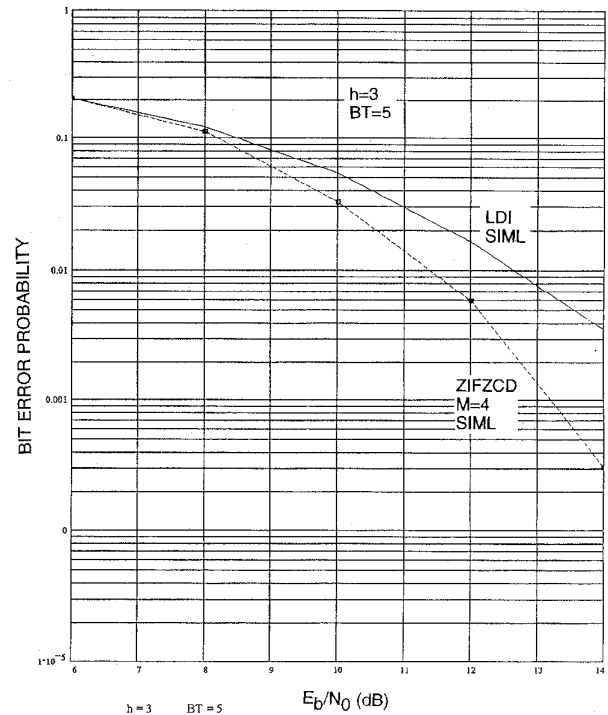

Fig. 6. BER of the ZIFZCD under static environment when $M = 4$. A wideband CPFSK with modulation index $h = 3$ and a Gaussian shape IF filter of $B_r T = 5$ were assumed.

computation should be divided into two parts as the "010" data pattern case in (48). For $M = 4$, the conditional BER, given a "110" data pattern, can be written as

$$P_b(E \mid \text{'110'})$$
$$= \frac{1}{\pi/M} \left\{ \int_0^{\pi/M - \Delta\phi_{110} + \pi} P_b(E \mid \text{'110'}, \phi_0, \text{Case}(1)) d\phi_0 \right.$$
$$\left. + \int_{\pi/M - \Delta\phi_{110} + \pi}^{\pi/M} P_b(E \mid \text{'110'}, \phi_0, \text{Case}(2)) d\phi_0 \right\}$$

$$(49)$$

where

$$P_b(E \mid \text{'110'}, \phi_0, \text{Case}(1)) = \bar{N}_{110} e^{-\bar{N}_{110}}$$
$$\times [1 - \{F_\psi(2(\Delta\phi_{110} - \pi) + \phi_0) - F_\psi(\Delta\phi_{110} - \pi)\}]$$
$$+ 1 - e^{-\bar{N}_{110}} - \bar{N}_{110} e^{-\bar{N}_{110}} + \frac{1}{2} \bar{N}_{110} e^{-\bar{N}_{110}}$$
$$\times \{F_\psi(2(\Delta\phi_{110} - \pi) + \phi_0) - F_\psi(\Delta\phi_{110} - \pi)\}$$
$$+ \frac{1}{2} e^{-\bar{N}_{110}} \{F_\psi(\pi/M - \phi_0) - F_\psi(\Delta\phi_{110} - \pi)\} \quad (50)$$

and

$$P_b(E \mid \text{'110'}, \phi_0, \text{Case}(2)) = \bar{N}_{110} e^{-\bar{N}_{110}}$$
$$\times [1 - \{F_\psi(2(\Delta\phi_{110} - \pi) + \phi_0) - F_\psi(\Delta\phi_{110} - \pi)\}]$$
$$+ 1 - e^{-\bar{N}_{110}} - \bar{N}_{110} e^{-\bar{N}_{110}} + \frac{1}{2} \bar{N}_{110} e^{-\bar{N}_{110}}$$
$$\times \{F_\psi(2(\Delta\phi_{110} - \pi) + \phi_0)$$
$$- F_\psi(2\Delta\phi_{110} - \pi) - (\pi/M - \phi_0)\}. \quad (51)$$

If M is 8, then $(\pi/M - \phi_0) \ (\leq 0.15\pi)$ is smaller than $\Delta\phi_{110} - \pi (= 0.19\pi)$. The integral interval with respect to ϕ_0 for the average BER computation is not necessary to be divided into two parts. The BER for $M \geq 8$ can be given by (41) with replacement of $\Delta\phi_{111}$ and $\bar{N}_{111}$ by $\Delta\phi_{110}$ and $\bar{N}_{110}$, respectively.

Using (40), (48), and (49), the overall bit error probability can be written as

$$P_b(E) = \frac{1}{4} \{P_b(E \mid \text{'111'}) + P_b(E \mid \text{'010'}) + 2P_b(E \mid \text{'110'})\}.$$

$$(52)$$

BER analysis will be performed in the future for the other case, i.e., a wideband digital FM signaling case with $h \geq 1.5$ under fading environment, because analysis is complicated. Only simulated BER results for this case will be presented in the next section.

V. NUMERICAL RESULTS

Fig. 5 shows both the analyzed and simulated BER results for the ZIFZCD under static environment when the number of phase axes M is 4, 8, and 16. An MSK signaling with $h = 1/2$ and a Gaussian IF filter of $B_r T = 1$ were assumed. The BER of the CDM (i.e., LDI) is also shown for comparisons. The analyzed and simulated results agree well. The required E_b/N_0 for the ZIFZCD to achieve the 10^{-2} BER is 13.3 dB from the simulated results while that of the CDM is 8 dB when M is 4. Thus, the ZIFZCD with $M = 4$ phase axes is 5.3 dB worse than the CDM. It is also observed that BER of the ZIFZCD improves as M increases. For example, when $M = 8$, the
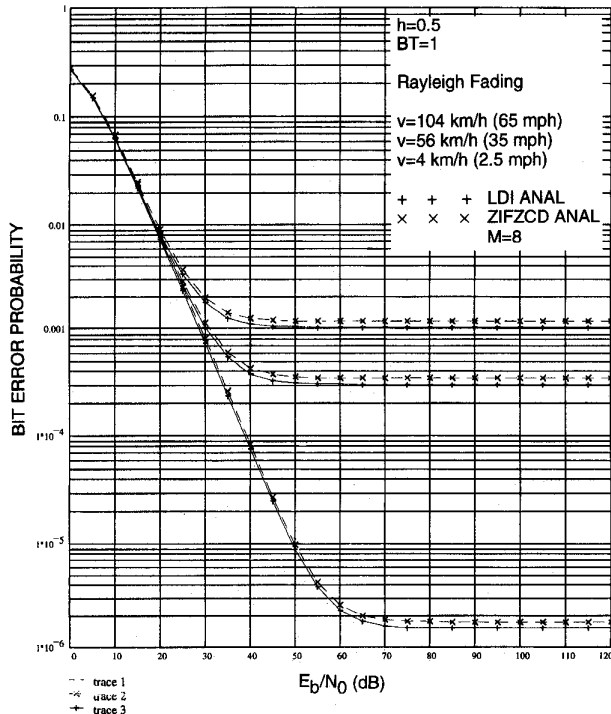
Fig. 7. BER of the ZIFZCD under fading environment when $M = 8$ phase axes and $v = 2.5$, 35, and 65 mph. A narrowband CPFSK signal with modulation index $h = 0.5$ and a Gaussian shape IF filter of $B_rT = 1$ were assumed.
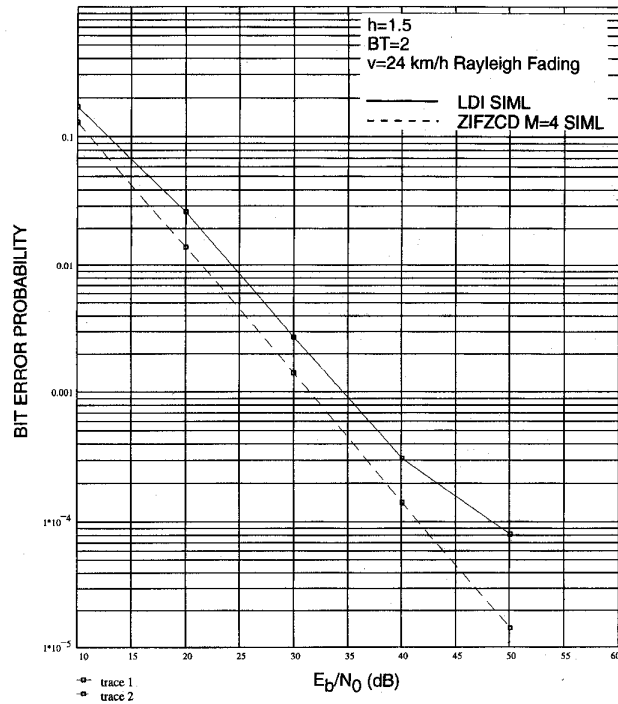

Fig. 8. BER of the ZIFZCD under fading environment when $M = 8$ phase axes and $v = 15$ mph. A wideband CPFSK with modulation index $h = 1.5$ and a Gaussian shape IF filter of $B_rT = 2$ were assumed.

ZIFZCD is only 1 dB worse than the CDM at 10^{-2} BER. The implementation of the ZIFZCD with $M = 8$ is still simpler than that of the CDM.

Fig. 6 shows the corresponding simulated BER results for the ZIFZCD under a static environment when $M = 4$, $h = 3$ and $B_rT = 5$. The simulated results indicate that the ZIFZCD can be 1.4 dB better than the CDM at 10^{-2} BER. This result is significant because the complexity of the ZIFZCD is simpler and BER performance is better than the CDM.

For BER demonstration under a fading environment, it is assumed that the data rate (R_b) is 11.52 kbps, carrier frequency $f_c = 1.8$ GHz, velocity of a mobile unit $v = 2.5$ mph ($= 4$ km/h), 35 mph ($= 56$ km/h), and 65 mph ($= 104$ km/h). The maximum Doppler frequency shift $f_D = vf_c/c$ would be 173 Hz when $v = 65$ mph, where c is the light velocity.

Fig. 7 shows the analyzed BER results for the ZIFZCD under a fading environment when $M = 8$, $v = 2.5$, 35, and 65 mph. An MSK signal with $h = 0.5$ and a Gaussian shape IF filter with $B_rT = 1$ were assumed. It is observed that the BER floor for the ZIFZCD with $M = 8$ axes is around 1.2×10^{-3} BER at $v = 65$ mph, which is generally acceptable for voice communications. The BER difference between the ZIFZCD and the CDM is insignificant (i.e., less than 0.5 dB) for all speeds when the ZIFZCD employs $M = 8$ axes. The simulated and analyzed results also agree well.

Fig. 8 shows the simulated BER for the ZIFZCD when $M = 4$ axes, $h = 1.5$, a Gaussian shape IF filter with $B_rT = 2$, and $v = 15$ mph (24 km/h). It is observed that the ZIFZCD is 3 dB better than the CDM at 10^{-3} BER under a fading environment. The digital FM with a large modulation

index is being employed in many systems, e.g., a paging [13] and a Motorola ALTAR in high-speed (15 Mbps) wireless local-area networks service [14]. It is a future topic to show theoretically why the ZIFZCD can be better than the CDM when digital FM modulation index is larger than 1.5 under both static and fading environments.

The relative BER degradation due to the presence of phase and gain imbalance between the I and Q phase axes was also analytically studied. The numerical results indicate that the relative degradation due to the I and Q phase imbalance is insignificant, e.g., 0.27 dB, if the phase imbalance is less than 5° for $M = 8$ axes and $v = 65$ mph. It was also observed that the relative BER degradation due to the presence of both phase and gain imbalance is insignificant, e.g., 0.5 dB if the I and Q phase imbalance is less than 5° and the I and Q gain imbalance is less than 5% for $M = 8$ axes and $v = 65$ mph.

In addition, the relative BER degradation due to the presence of a frequency offset was analytically studied. It was observed that the relative degradation due to the frequency offset is 1.45 dB and 4.8 dB when the frequency offset is 3% and 6% of the data rate, respectively. If a frequency offset is less than 3% of the data rate, the relative degradation is insignificant. A device which can reduce the frequency offset effects is required if the frequency offset is larger than 3%. One simple frequency offset compensation scheme is to estimate the frequency offset by measuring a d.c. value of the zero-crossing counter outputs, and to subtract the estimated d.c. value from the zero-crossing counter output. This function is similar to that of the d.c. block scheme in the conventional LDI in order to reduce the effects of the frequency offset.

VI. CONCLUSION

A novel digital FM receiver, called ZIFZCD, was introduced. The implementation of the ZIFZCD is significantly simpler than that of the conventional CDM because the ZIFZCD is based on binary addition and binary multiplication while that of the CDM on real addition, multiplication, differentiation, and division. Therefore, the ZIFZCD scheme meets the digital IC implementation requirements much better than the CDM for wireless communication systems.

It was observed that the BER performance of the ZIFZCD under both static and fading environments is comparable to that of the CDM for a narrowband digital FM with modulation index 0.5. For example, when $M = 4$ and 8 phase axes are employed, the ZIFZCD is only 1 dB and 0.5 dB worse than the CDM at 10^{-2} BER under static and fading environments, respectively.

In addition, it was observed that the BER performance of the ZIFZCD with even a small number of phase axes, such as $M = 4$, can be significantly better than that of the conventional CDM when a wideband digital FM signal with modulation index larger than 1.5 is employed. These results indicate that the ZIFZCD may be well suited for paging systems or high-speed wireless local-area networks with high digital FM modulation indices.

Finally, it was also observed that the relative BER degradation due to the frequency offset, the I-Q phase, and I-Q gain imbalances, are insignificant when the frequency offset and imbalances are within practical ranges.

ACKNOWLEDGMENT

The authors would like to thank the anonymous reviewers for their helpful and constructive comments.

REFERENCES

[1] "Digital European cordless telecommunication common interface," *ETS 300175*, European Telecommunication Standards Institute, Mar. 1992.
[2] I. Vance, "Decoding logic for frequency shift keying receiver," U.S. Patent 4322851, Mar. 30, 1982.
[3] J. Park, "An FM detector for low S/N," *IEEE Trans. Commun.*, vol. COM-18, no. 2, pp. 110–118, Apr. 1970.
[4] H. Meyr and R. Subramanian, "Advanced digital receiver principles and technologies for PCS," *IEEE Commun. Mag.*, pp. 68–78, Jan. 1995.
[5] G. Boscagli, M. C. Comparini, and M. Martone, "Digital receiver for on-board FM/FSK-FM/BPSK demodulation," in *5th NASA Symposium on VLSI Design*, New Mexico University, 1993, pp. 3.4.1–3.4.13.
[6] E. K. B. Lee, "Communication device with zero-crossing demodulator," U.S. Patent Filed, May 5, 1994.
[7] E. K. B. Lee and J. P. Heck, "Communication device with efficient zero-crossing generator," U.S. Patent Filed, Apr. 1994.
[8] P. Estabrook and B. Lusignan, "The design of a mobile radio receiver using a direct conversion architecture," in *IEEE 39th Veh. Technol. Conf.*, 1989.
[9] C. S. Ng, T. T. Tjhung, F. Adachi, and F. P. S. Chin, "Closed-form error probability formula for narrow-band FSK, with limiter-discriminator-integrator detection, in Rayleigh fading," *IEEE Trans. Commun.*, vol. 42, no. 10, pp. 2795–2802, Oct. 1994.
[10] R. F. Pawula, "On the theory of error rates for narrow-band digital FM," *IEEE Trans. Commun.*, vol. COM-29, no. 11, pp. 1634–1643, Nov. 1981.
[11] E. K. B. Lee, C. Powell, and H. Kwon, "A novel wireless communication device with synchronized zero-crossing demodulator," in *IEEE GLOBECOM'95*, Singapore, Nov. 13–17, 1995, U.S. Patent Filed, July 1995.
[12] R. F. Pawula, "Refinements to the theory of error rates for narrow-band digital FM," *IEEE Trans. Commun.*, vol. 36, no. 4, pp. 509–513, Apr. 1988.
[13] R. H. Tridgell, "Standard message formats for digital radio paging," *British Telecom.*, Autumn 1980.
[14] J. A. Wepman, "Analog-to-digital converters and their applications in radio receivers," *IEEE Commun. Mag.*, vol. 33, no. 5, pp. 39–45, May 1995.
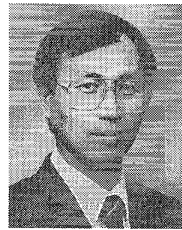
Hyuck M. Kwon (S'82–M'84–SM'96) was born in Korea on May 9, 1953. He received the B.S. and M.S. degrees in electrical engineering from Seoul National University, Seoul, Korea, in 1978 and 1980, respectively, and the Ph.D. degree in computer, information, and control engineering from the University of Michigan, Ann Arbor, in 1984.

While at the University of Michigan, he worked as a Research Assistant at Cooley Electronic Laboratory. From 1985 to 1989, he was with the University of Wisconsin, Milwaukee, WI, as an Assistant Professor in the electrical engineering and computer science department. From 1989 to 1993, he was with the Lockheed Engineering and Sciences Company, Houston, TX, as a Principal Engineer, where he was responsible for analysis of the Space Station Freedom and Space Shuttle communication systems. Since 1993, he has been with Wichita State University, Wichita, KS, as a Faculty Member in the electrical engineering department. In addition, he served as a Summer Visiting Professor for J. S. Lee Associates, Inc., Arlington, VA, in 1987, Motorola Paging Product Groups Research Laboratory, Boynton Beach, FL, in 1994, and Samsung Information Systems America, San Jose, CA, in 1996, where he studied the narrowband digital FM spread-spectrum, paging, IS-95 code division multiple access mobile communication systems, respectively. His current interests include global system for mobile, satellite, and personal communication systems.

Kwang Bok (Ed) Lee (M'96) received the B.A.Sc. and M.Eng. degrees from the University of Toronto, Canada, in 1982 and 1986, respectively, and the Ph.D. degree from McMaster University, Canada, in 1990.

He was with Motorola Canada from 1982 to 1985, and Motorola USA from 1990 to 1996 as a Senior Staff Engineer. In Motorola, he was involved in the research and development of various communication systems. He was with Bell-Northern Research in Canada from 1989 to 1990. In March 1996, he joined the School of Electrical Engineering at Seoul National University in Korea as an Assistant Professor. His research interests include communication theories, communication systems, and adaptive signal processing. He holds eight U.S. patents and has two U.S. patents pending.